Discover Oncology

Research

Identification and construction of prognostic clusters and risk-prognosis model based on aging-immune related genes in bladder cancer

Nihao Cao[1] · Fei Cheng[1] · Jincai Zhou[2] · Ning Liu[3]

Received: 12 July 2024 / Accepted: 28 November 2024
Published online: 04 December 2024
© The Author(s) 2024 OPEN

Abstract

Background Faced with the current global ageing situation, advanced age has become a risk factor for bladder carcinogenesis progression and immunotherapy. Exploring the common mechanisms of aging and immune in bladder cancer and finding new prognostic markers and immunotherapeutic targets has become an urgent issue.

Method Aging-immune related genes (AIGs) were collected from the public databases MSIGDB, HAGR and ImmPort, and hub AIGs were finally identified in the TCGA-BLCA disease cohort by expression, prognosis, and clinicopathological correlation analysis, and the correlation of hub AIGs with immune microenvironment, immunotherapeutic response, ferroptosis and m6A methylation was verified. Subsequently, prognostic clusters and risk-prognosis models for AIGs was constructed by cluster analysis and multifactorial Cox regression analysis, and the gene mutation and immune infiltration characteristics of the different clusters were explored. Finally, the expression level of related genes was verified by immunohistochemical experiments using patient samples from our medical center.

Result 145 potential prognostic AIGs were collected in bladder cancer and finally clarified NFKB1 and IL7 with significant expression differences, prognostic value and age correlation. By single gene analysis, hub AIGs were explored to be significantly correlated with immunotherapeutic response, immune microenvironment, ferroptosis and m6A methylation. Subsequently, the risk-prognosis model was constructed with Riskscore = (0.0581)*NFKB1 + (− 0.2285)*IL7. And prognostic clusters based on hub AIGs was performed by cluster analysis, which clarified that the high-risk group was the pro-cancer group, which had a lower mutation rate of hub genes and higher of neutrophil infiltration. Finally, immunohistochemistry of patients confirmed that IL7 and NFKB1 were underexpressed in bladder cancer, and the proliferation and migration ability of tumor cells were significantly decreased after overexpression of these genes.

Conclusion This study is the first to identify NFKB1 and IL7 as hub AIGs in bladder cancer, which provide new prognostic markers and immunotherapeutic targets.

Keywords Aging-immune · Bladder cancer · Prognostic model · Immune microenvironment · NFKB1-IL7

Nihao Cao and Fei Cheng contributed equally.

Supplementary Information The online version contains supplementary material available at https://doi.org/10.1007/s12672-024-01655-0.

✉ Jincai Zhou, 13651591579@163.com; ✉ Ning Liu, liuningseu@163.com; Nihao Cao, 773989100@qq.com; Fei Cheng, 893112427@qq.com | [1]Department of Urology, Nantong Haimen People's Hospital, Nantong 226100, China. [2]Department of Urology, Jianhu People's Hospital, Jianhu County, No. 666 South Ring Road, Yancheng 224700, China. [3]Department of Urology, Zhongda Hospital, Southeast University, No. 87 Dingjiaqiao, Hunan Road, Gulou District, Nanjing 210009, China.

1 Introduction

Bladder cancer (BLCA) ranked 12th in the 2020 Global Cancer Statistics with 573,278 new cases, accounting for 3.0% of new cancer cases, and 212,536 new deaths, accounting for 2.1% of new cancer deaths [1]. BLCA, the second most common malignancy of the genitourinary system, has a high recurrence rate (30–70%) [2] and high invasiveness (30%) [3], which is divided into non-muscle invasive bladder cancer (NMIBC) and non-muscle invasive bladder cancer (MIBC). According to existing studies, advanced age (70–84 years) [4], smoking [5], chronic inflammation [6], pelvic radiotherapy [7] and genetic factors [8] were risk factors for BLCA. The 5-year progress free interval (PFI) rate after treatment for NMIBC was poor according to low, intermediate and high risk stage [9]. For MIBC, although mitomycin C and BCG improved PFI and overall survival (OS), the results were not satisfactory and accompanied with fatal adverse effects [10, 11]. Age was now accepted as the single largest risk factor for the development of BLCA [12]. Studies showed that BLCA could occur at any age, with a median age at diagnosis of approximately 70 years [12]. For patients aged 65–69 years, the incidence of BLCA was approximately 142 per 100,000 men and 33 per 100,000 women, while for patients aged ≥ 85 years, the incidence was approximately 296 per 100,000 men and 74 per 100,000 women [13]. Related studies further found that age could influence the efficacy of intravesical treatments, particularly immunotherapy. The absolute difference in 5-year PFI after intravesical BCG was 10% in patients < 70 (37%) compared to patients > 70 (27%) [14]. Additionally, absolute PFI was 22% lower in patients ≥ 80 years old treated with BCG plus interferon compared to those aged 60–70 years [15]. The above study demonstrated how advanced age is not only a risk factor for the development of BLCA, but also a key factor affecting its immunotherapy.

Bladder cancer was predicted to be a great social challenge facing the dire situation of the ageing society. Therefore, exploring the common mechanisms of ageing and immune and seeking new prognostic markers and immunotherapeutic targets had become a pressing issue. Professor Walford in 1969 proposed immunosenescence, which referred to the deterioration of the immune system, including immune organs and immune cells, with increasing age. Professor T. J. Newman further constructed an age-related model of T-cell production [16], and Professor D. Monti also pointed out that the main features of immunosenescence include thymic degeneration, reduced number and diversity of T cells, reduced antigen-presenting capacity of dendritic cells, reduced phagocytosis of macrophages, and an increase in myeloid-derived suppressor cells (MDSCs), leading to decreased immune surveillance and cancer cell clearance, and ultimately to proliferation, metastasis and drug resistance of cancer cells [17]. Comprehensive of the existing literatures, only Prof. Liu explored the prognostic model under immunosenescence-related typing in BLCA by a simple clustering approach and extended it to pan-cancer [18], however, their study did not further identify specific hub immunosenescence genes or explore their correlation with tumour immune microenvironment, etc.

In this study, AIGs were collected from the public databases MSIGDB, HAGR and ImmPort, and genes were identified in the TCGA-BLCA disease cohort by expression and prognostic analysis, and hub AIGs were finally identified by clinicopathological correlation analysis, which were verified to be associated with immune microenvironment, immunotherapeutic response, ferroptosis and m6A methylation. Subsequently, prognostic clusters and risk-prognosis models of AIGs were constructed by cluster analysis and multifactorial Cox regression analysis, and the mutation and immune infiltration characteristics under different clusters were explored in depth.

2 Method

2.1 TCGA-BLCA data, aging-immune related genes download

mRNA expression and clinicopathological data for BLCA were downloaded from the TCGA database (https://portal.gdc.cancer.gov/); a total of 598 human aging-related genes were downloaded from the MSIGDB (https://www.gsea-msigdb.org/gsea/msigdb/index.jsp/) and the HAGR (http://genomics.senescence.info/genes/) database; 1793 immune-related genes were obtained in the Immunology Database and Analysis Portal (ImmPort) database (https://www.immport.org/home).

2.2 Gene differential expression, survival prognosis, clinicopathological analysis

Differential expression, OS, PFS and disease specific survival (DSS) of AIGs in the TCGA-BLCA cohort were analyzed using the "survival R package". Correlation of hub AIGs with clinicopathological features was investigated based on the "survival R package", and prognostic overall survival K-M curves and calibration curves were plotted.

2.3 Prognostic nomogram and risk-prognostic model

Prognostic nomogram based on hub AIGs was constructed using the 'rms' package to predict the OS of bladder cancer at 1, 3 and 5 years. Moreover, risk-prognosis model was constructed using multifactorial Cox regression analyzes. Finally, the validity of the prognostic model was evaluated using the area under the curve (AUC) of the "time subject operating characteristic" (ROC). Spearman correlation analysis was used to explore the relationship between model scores and immune scores.

2.4 Immunocorrelation analysis of hub AIGs

Tumor mutation load (TMB) scores were calculated using Perl scripts and then corrected by total exon length, followed by analysis of hub gene expression in relation to TMB using Spearman correlation coefficients. The Tumor Immune Dysfunction and Exclusion (TIDE) algorithm was used to assess the potential ICB response to immune checkpoint inhibitors at hub AIGs expression levels. The relationship between immune checkpoint-related genes such as SIGLEC15, TIGIT, CD274, HAVCR2, PDCD1, CTLA4, LAG3 and PDCD1LG2 and hub AIGs expression was analyzed using the "ggplot2" R package. The xCELL algorithm was used to determine the correlation between hub AIGs expression and the immune infiltrative microenvironment of bladder cancer. Dryness scores were obtained from tumour-associated RNA-seq data by TCGA-BLCA and mRNAsi by the OCLR algorithm.

2.5 Analysis of ferroptosis and m6A methylation-associated genes

RNA sequencing data of the genes were obtained based on the TCGA dataset and analysed for correlation with the ferroptosis and m6A methylation-associated genes in the "ggplot2" R package.

2.6 Cluster analysis

Cluster analysis was carried out using the Consensus Cluster Plus R package, using 1-pearson correlation distance clustering PAM, with 10 replicate resamplings of 80% of the samples. The optimal number of clusters was determined using empirical cumulative distribution function plots.

2.7 Identification of differential expressed genes

Differential mRNA expression between clusters was analyzed using the Limma package (version: 3.40.2). mRNA differential expression was screened for adjusted $P < 0.05$ and $|\text{fold change}| > 1$.

2.8 Functional enrichment and gene enrichment analysis

Gene Ontology (GO) and the Kyoto Encyclopedia of Genes and Genomes (KEGG) were used to assess functional enrichment analysis of aging-immune related genes and different clusters using the "clusterProfiler" software package, provided that the q-value < 0.05 and p-value < 0.05. In addition, differences in genesets of different aging-immune disease clusters were further assessed based on GSEA software (http://www.broadinstitute.org/gsea/index.jsp).

2.9 Somatic mutation and immune landscape analysis

BLCA somatic mutation data were obtained from the TCGA GDC data Portal and waterfall plots were created by the "Maftools" software package. The relative percentages of various immune cell types were determined using the xCELL, TIMER, quanTIseq, CIBERSORT and EPIC algorithms, and the relative percentages of immune cell types between two clusters were compared using a landscape sample.

2.10 Cell lines and culture

Human BCa cell line (UMUC3) was obtained from the surgical laboratory of Zhongda Hospital, Southeast University, and were provided by Dr. Ning Liu. UMUC3 was cultured in DMEM medium, containing 10% fetal bovine serum, and 1% penicillin–streptomycin solution.

2.11 Cell phenotype

For cell proliferation assay, 1000 cells were seeded into 96-well plates for 0–96 h, and 10 µL of the cell counting kit-8 solution was added per well. After a 2-h incubation at 37 °C, optical density (OD) at 450 nm was measured on a microplate reader. For the colony formation assay, cells were seeded into 6-well plates at a density of $1–2 \times 10^3$ cells/well and incubated for 10–14 d at 37 °C. Cells were inoculated onto 6-well plates for the wound-healing assay and treated with oe-/nc-IL7 and oe-/nc-NFKB1. The cell wound edge was marked and photographed under a microscope at the starting time point, and after 0–24 h, the cells' migrated distances were measured and analyzed for the wound closure percentage. For migration assays, cells were inoculated into a 24-well transwell cell apical chamber for evaluating cell invasion. Cells that invaded the bottom chambers were fixed with 4% polyformaldehyde, stained with 0.1% crystal violet solution, counted, and photographed under a microscope.

2.12 Immunohistochemical staining

The formalin-fixed paraffin-embedded tissue was dewaxed and dehydrated using xylene and serially-diluted ethanol. The tissue sections were incubated at 121 °C in an autoclave for 5 min to extract the antigen, then incubated with IL7 and NFKB1 monoclonal antibody at 4 °C overnight, and the bound antibody was incubated at 37 °C for 30 min. The bound antibody was detected using 3,3′-diaminobenzidine-kit and hematoxylin.

2.13 Statistical analysis

Statistical analyses for this study were performed automatically by the relevant databases. Differences were statistically significant when $p < 0.05$ or log rank $p < 0.05$.

3 Result

3.1 Identification of five prognostic AIGs in the TCGA-BLCA

All 145 genes were identified as co-expressed AIGs by Venn diagram (Fig. 1A). 33 genes were found to have potential prognostic value by univariate Cox regression analysis (Supplementary Fig. 1). Unfortunately, however, of these 28 genes, AGER, CTSS, IGF2, EGFR, EPOR, and IKBKB were not differential expressed in bladder cancer versus paraneoplastic + normal tissue (Supplementary Fig. 2A–G), and CALCA, CCN2, EDNRB, JUN, LRP1, PENK, TGFB3, IL33, S100A6, GHR PTPN11, IGF1, NGF, NGFR, NR3C1, A2M, FGFR1, ELN, PPARG, AGTR1 and PDGFRA whose expression levels of contradicted the prognostic status (Supplementary Fig. 2A–G). Ultimately, GBP2, PLCG2, NFKB1, PTK2B and IL7 were found to be lowly expressed in bladder cancer by unpaired expression analysis (Fig. 1B), and PLCG2, NFKB1 and IL7 were also lowly expressed in paired expression analysis (Fig. 1C). Low expression of the above five genes in BLCA was correlated with poor OS by prognostic

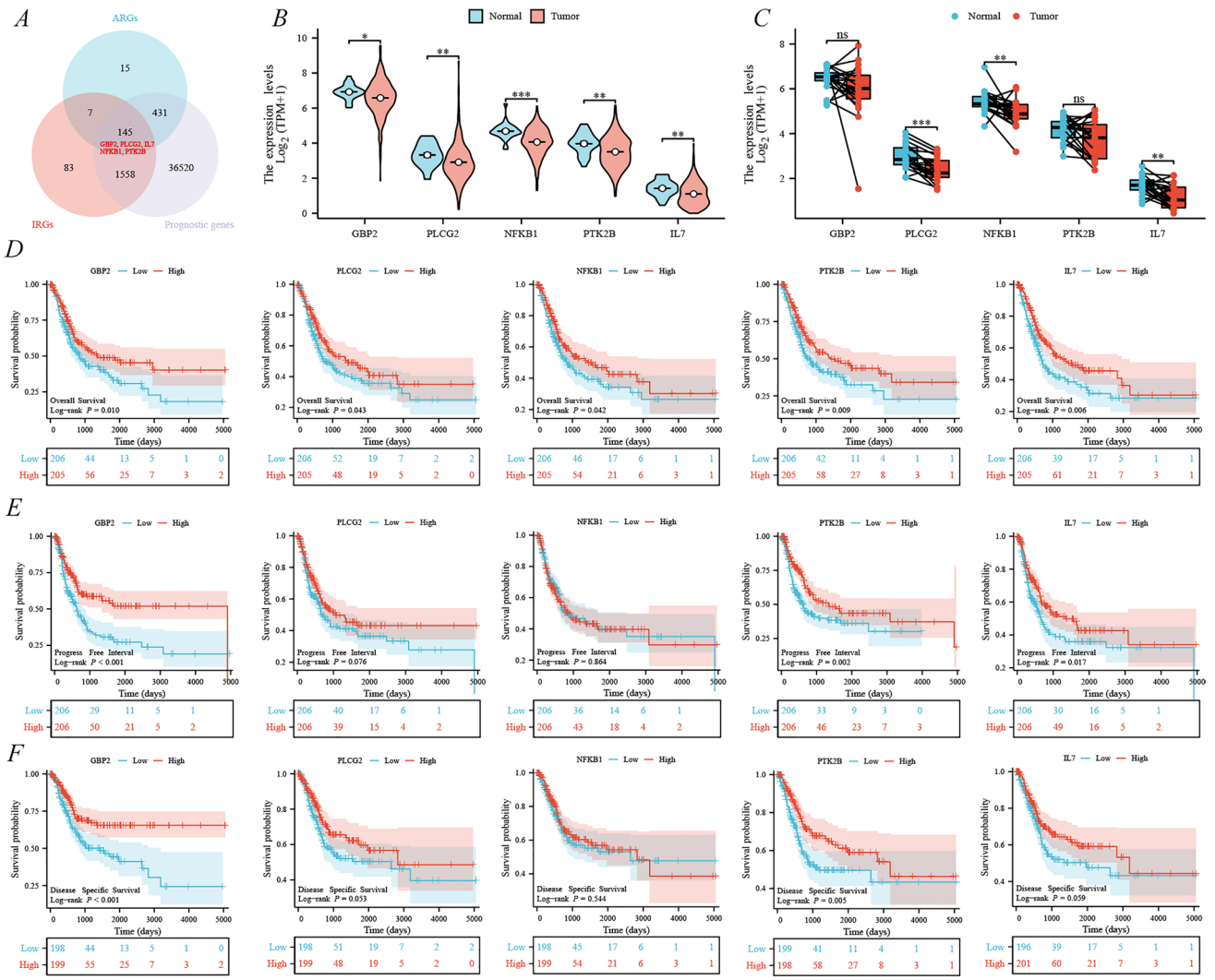

Fig. 1 Identification of five aging-immune related genes in the TCGA-BLCA cohort. **A** Preliminary screening of potential prognostic AIGs by Venn diagram; unpaired expression (**B**) and paired expression (**C**) of GBP2, PLCG2, NFKB1, PTK2B, IL7; overall survival (**D**), progress free interval (**E**) and disease-specific survival (**F**) of GBP2, PLCG2, NFKB1, PTK2B, IL7

K-M plots ($p < 0.05$) (Fig. 1D), and moreover, low expression of GBP2, PTK2B and IL7 was associated with poor PFI and poor DSS (Fig. 1E, F). Collectively, this study initially identified GBP2, PLCG2, NFKB1, PTK2B and IL7 as tumor suppressor gene with significant prognostic value in BLCA.

3.2 Identification of pathway enrichment for co-expression AIGs

By STING, the protein interaction network of 35 co-expressed AIGs was identified, as well as EGFR, VEGFA, IGF1, CTGF and JUN were found to be at the centre of the network (Fig. 2A). Through GO analysis, the above genes were found to be enriched in positive regulation of MAPK cascade, response to peptide and positive regulation of fibroblast proliferation, regulation of epithelial cell proliferation, neuroinflammatory response (BP); vesicle lumen, platelet alpha granule, collagen-containing extracellular matrix, transport vesicle, CD40 receptor complex (CC); Signaling receptor activator activity, integrin binding, protein serine/threonine/tyrosine kinase activity, according to the protein binding and G protein-coupled receptor binding (MF), whose the p.adjust < 0.05 and qvalue < 0.05 (Fig. 2B). KEGG analysis showed that the functions enriched in MAPK signaling pathway, Proteoglycans in cancer, Chemical carcinogenes-reactive oxygen species, and PD-L1 expression and PD-1 checkpoint pathway in cancer, Leukocyte transendothelial migration, Prostate cancer and Renal cell carcinoma et al. (Fig. 2C). Subsequently, further analysis of the five tumor suppressor genes with significant prognostic value revealed weak correlations for GBP2, PLCG2, NFKB1, PTK2B and IL7, with NFKB1 at the centre (Fig. 2D).

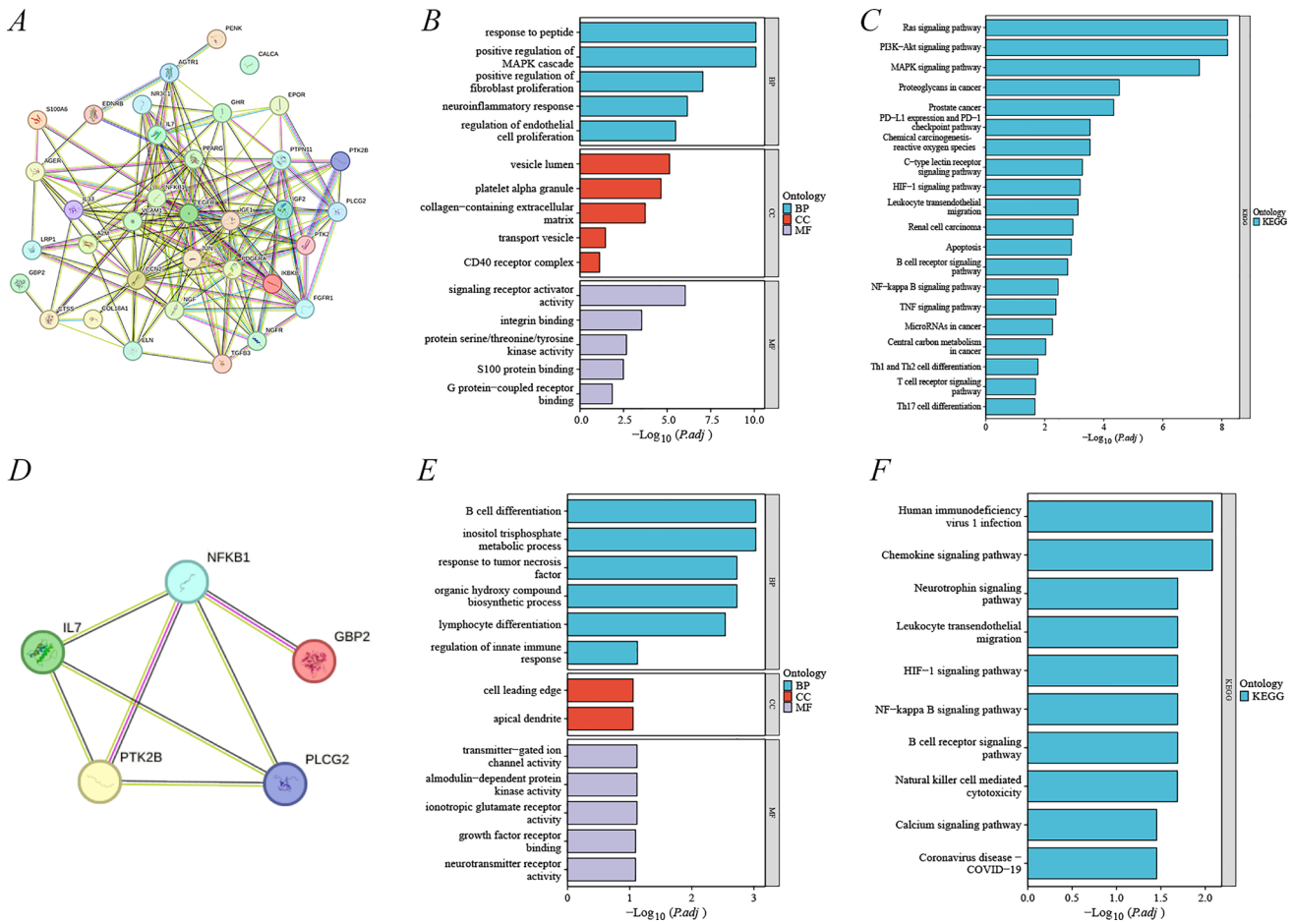

Fig. 2 Identification of pathway enrichment for aging-immune related genes. 35 protein interaction networks co-expressing AIGs (**A**), GO (**B**) and KEGG (**C**) analysis; protein interaction networks for five AIGs (**D**), GO (**E**) and KEGG (**F**) analysis

The GO-KEGG analysis of the above genes indicated that they were mainly enriched in B cell differentiation, response to tumor necrosis factor and lymphocyte differentiation (BP); apical dendrite, cell leading edge (CC); growth factor activity, ionotropic glutamate receptor activity (MF); Chemokine signaling pathway, NF – kappa B signaling pathway, B cell receptor signaling pathway (KEGG), whose the p.adjust < 0.05 and qvalue < 0.05 (Fig. 2E, F).

3.3 Correlation of the hub AIGs NFKB1 and IL7 with the BLCA clinicopathological features

In the TCGA-BLCA disease cohort, low expression of NFKB1 and IL7 was found to be associated with the development of lymph node metastasis (N1&2&3) and distant metastasis (M1) (Fig. 3B, C). Additionally, low expression of PLCG2 and PTK2B was associated with the development of lymph node metastasis (N1&2&3) (Fig. 3B) and low expression of GBP2 was associated with high T-stage (T3&4) (Fig. 3A). Low expression of PLCG2 and PTK2B correlated with high stage (Stage III&IV) and high grade (Fig. 3E, F). Notably, using 70 years as the advanced age cut-off, only NFKB1 and IL7 were significantly underexpressed in advanced age patients (> 70 years) (Fig. 3D). The remaining clinicopathological features with NFKB1 and IL7 were shown in Supplementary Table 1. Combined with the study objectives and the correlation between paired analyzes and clinicopathological features, this study tentatively identified NFKB1 and IL7 as hub AIGs in bladder cancer. Further exploration revealed 1,3,5 year diagnostic AUC curves of 0.428,0.482 and 0.443 for NFKB1, and 0.372,0.428 and 0.448 for IL7 respectively (Fig. 3G), as well as the time dependent AUC curves for NFKB1 and IL7 are shown in Fig. 3H. Interestingly, after combined age groups, the diagnostic AUC curves for NFKB1 and IL7 were significantly higher at 0.595 and 0.582 respectively (Fig. 3I). Therefore, the study constructed a prognostic nomogram of the three elements of NFKB1, IL7 and age with concordance = 0.592, p < 0.05 (Fig. 3J), and its 1,3,5 year prognostic calibration curve was well fitted to the ideal curve, especially for 3 years (Fig. 3K). By K-M curves, high expression of this combined indicator was found to

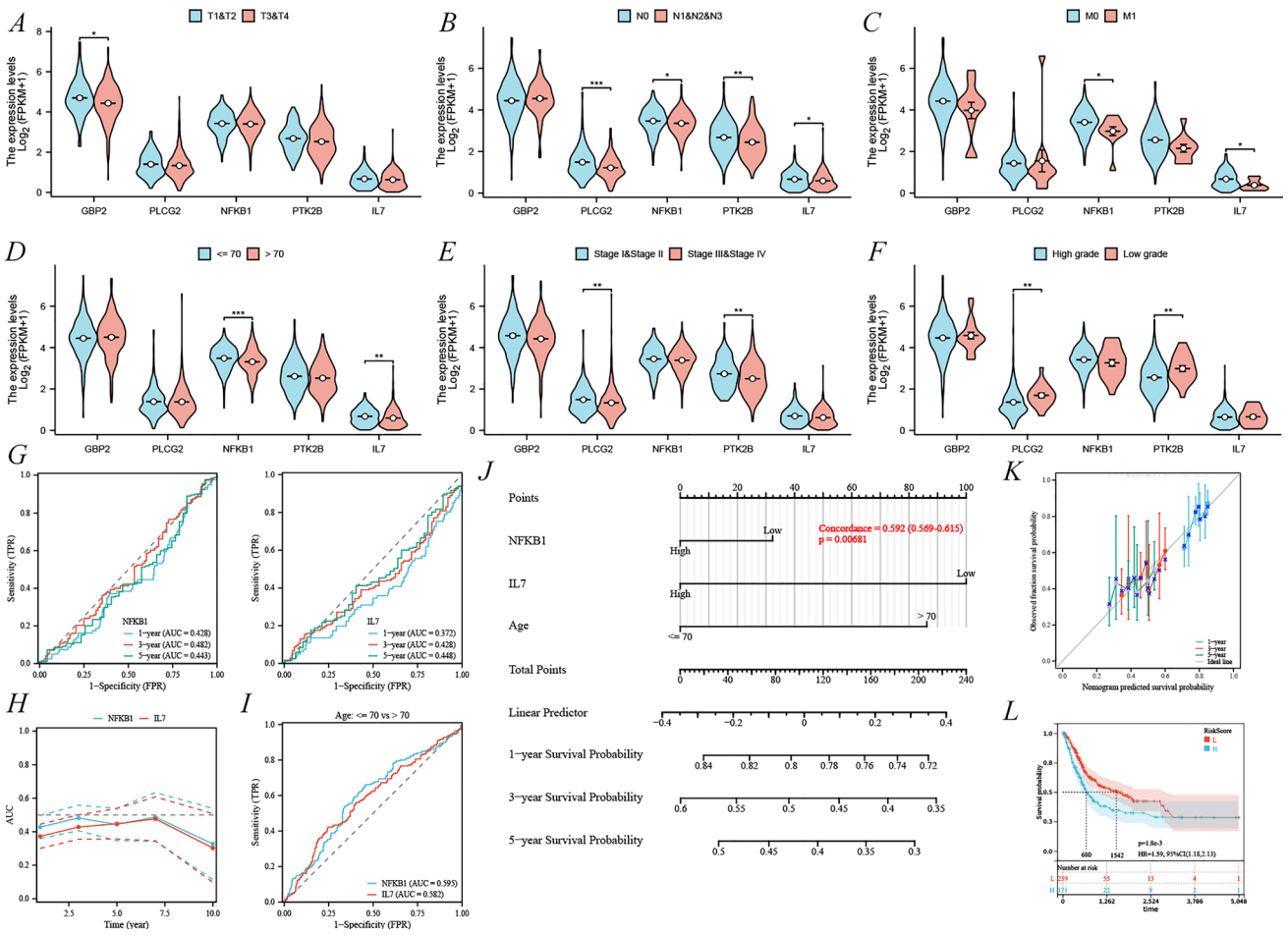

Fig. 3 Association of aging-immune related genes with clinicopathological features. Correlation of five AIGs with T (**A**), N (**B**), M (**C**), age (**D**), stage (**E**) and grade (**F**); **G** 1,3,5 year diagnostic AUC curves for NFKB1 and IL7; **H** time dependent AUC curves; **I** diagnostic AUC curves for NFKB1 and IL7 combined with age; **J** prognostic nomogram for NFKB1, IL7 combined with age; **K** prognostic calibration curves; **L** overall survival

be significantly associated with poor OS, showing a pro-carcinogenic effect (Fig. 3L), which would be somewhat contradicted by the initial diagnosis of NFKB1 and IL7 as suppressor genes in bladder cancer (Fig. 1B, D, 3A–F). In order to reconfirm in the expression of IL7 and NFKB1 in bladder cancer, the GSE121711, GSE45184 and GSE3167 datasets were used in this study. In GSE3167, IL7 was significantly under-expressed in tumor patients, while the trend in GSE121711 and GSE45184 was not statistically significant (Supplementary Fig. 3A–C); In GSE121711, NFKB1 was significantly under-expressed in tumor patients, while the trend in GSE45184 was not statistically significant (Supplementary Fig. 3D, E). The above results were consistent with the TCGA-BLCA results, which demonstrated that IL7 and NFKB1 were lowly expressed in bladder cancer.

3.4 Investigation of the correlation between hub AIGs with immune infiltration, ferroptosis and m6A methylation

A negative correlation between NFKB1 expression and TMB score was found ($p_{Spearman} = 0.12$, $p < 0.05$), while there was no correlation for IL7 (Fig. 4A). TIDE scores were lower in patients with low NFKB1 expression by ICB response analysis, who had good immune checkpoint blockade (ICB) therapy efficacy and longer survival, while there was no correlation with IL7 (Fig. 4B). Further exploration of the relationship between NFKB1 and IL7 and immune checkpoint-related genes revealed that the NFKB1 low expression group (G1) had significantly lower expression of CD274, CTLA4, HAVCR2, LAG3, PDCD1, PDCD1LG2 and TIGIT and higher expression of SIGLEC15 (Fig. 4C); the IL7 low expression group (G1) had significantly lower expression of CD274, CTLA4, HAVCR2, LAG3, PDCD1, PDCD1LG2 and TIGIT (Fig. 4C). Subsequently, the correlation

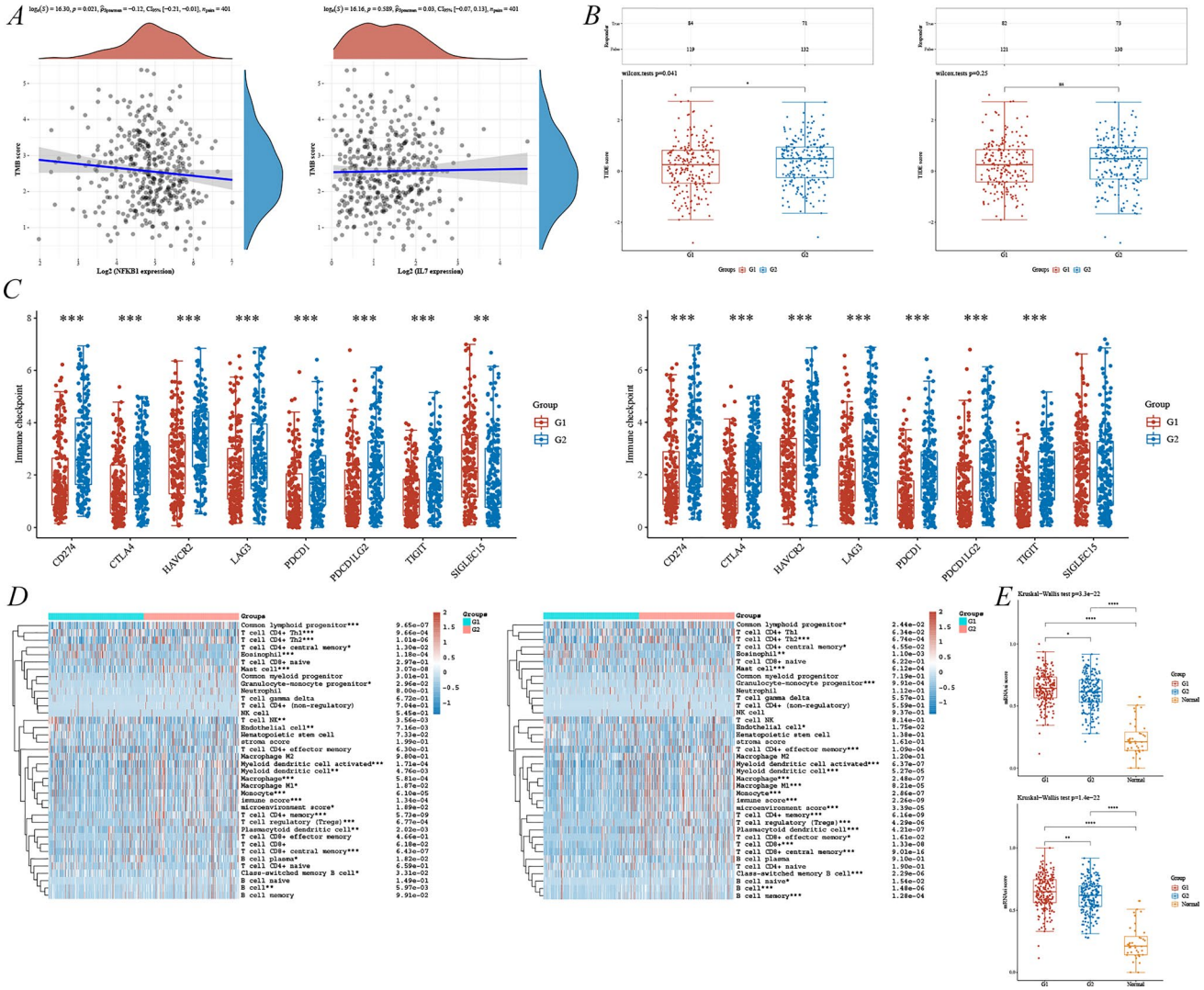

Fig. 4 Immunological correlation analysis of NFKB1 and IL7. **A** Correlation of NFKB1 and IL7 with TMB scores; **B** ICB response; **C** immune checkpoint-associated genes; **D** immune infiltration heat map under the xCELL algorithm; **E** dryness score. C1 gene low expression group, C2 gene high expression group

between NFKB1 and IL7 expression and immune infiltration was assessed by the xCELL algorithm suggesting that the NFKB1 low expression group (G1) had elevated T cell CD4+Th1, Eosinophil, T cell NK infiltration, while T cell CD4+Th2, Mast cell, Macrophage Monocyte, T cell CD4+ memory, and T cell regulatory infiltrates were low (Fig. 4D). In contrast, T cell CD4+Th2, Mast cell, T cell CD4+ effector memory, Myeloid dendritic cell activated, Macrophage, Macrophage M1, Monocyte, T cell CD4+ memory, T cell regulatory, T cell CD8+, B cell infiltration are low in the IL7 low expression group (G1) (Fig. 4D). Subsequently, the dryness score revealed a significantly higher degree of dryness in the NFKB1 and IL7 low expression group (G1) than in the high expression group (G2) and the normal group (Fig. 4E).

Subsequently, the ferroptosis-related genes SLC7A11, ATP5MC3, ACSL4, ATL1, NFE2L2, NCOA4, PCAT3, EMC2, CS, HSPA5, CARS1, CISD1, SAT1, DPP4, and CDKN1A were explored to be less expressed in the NFKB1 low expression group (G1) (Fig. 5A). SLC7A11, ACSL4, NFE2L2, NCOA4, LPCAT3, EMC2, HSPA5, CISD1, SAT1, DPP4, and CDKN1A were significantly lower in the IL7 low expression group (G1) (Fig. 5B). Meanwhile, most of the m6A methylation-related genes in the NFKB1 low expression group (G1) showed a significant low expression, except for METTL3 and IGF2BP1 which were not significant (Fig. 5C); the situation within the IL7 low expression group (G1) was similar (Fig. 5D).

To further clarify the signaling pathways of NFKB1 and IL7 in bladder cancer, this study performed single-gene GSEA pathway enrichment analysis of IL7 and NFKB1, respectively. The correlation results suggested that there were multiple identical pathways for IL7 and NFKB1, such as immunotherapy-associated pathways (e.g.,

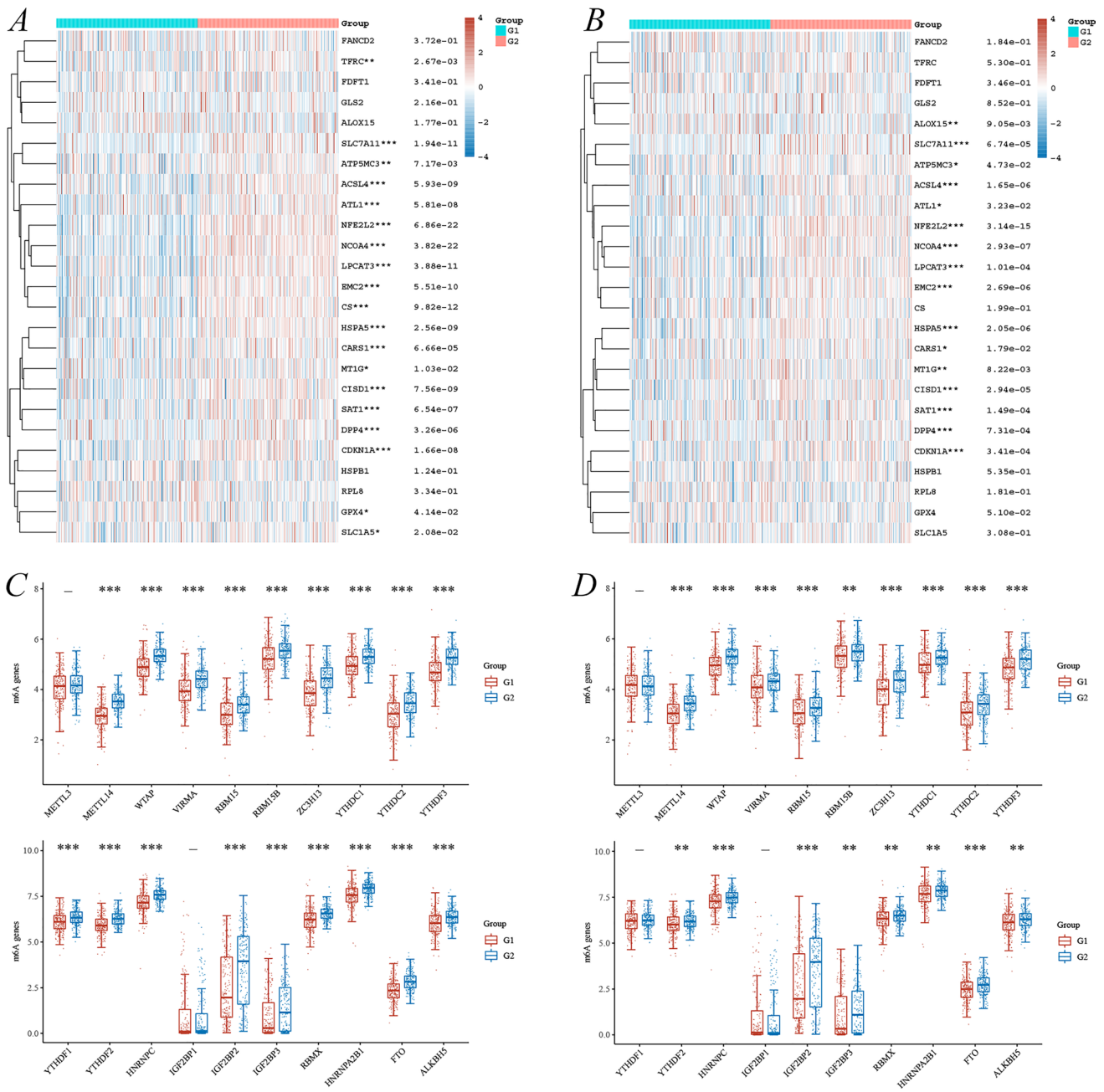

Fig. 5 Correlation of NFKB1 and IL7 with ferroptosis and m6A methylation. **A** Ferroptosis-related genes; **B** m6A methylation-related genes. C1 gene low expression group, C2 gene high expression group

CANCER_IMMUNOTHERAPY_BY_PD1 AND CTLA4_BLOCKADE), various immune cell-associated pathways (e.g., IMMUNOREGULATORY_INTERACTIONS_BETWEEN_A_LYMPHOID_AND_A_NON_LYMPHOID_CELL, NEURAL_CREST_CELL_MIGRATION_IN_CANCER, and NATURAL_KILLER_CELL_MEDIATED_CYTOTOXICITY), and critical signaling pathways (e.g., JAK_STAT_SIGNALING_PATHWAY, INTERFERON_SIGNALING, andPI3K_AKT_SIGNALING_IN_CANCER) (Supplementary Fig. 4A, B).

3.5 Construction of aging-immune related prognostic clusters and risk-prognosis models

As only two genes, NFKB1 and IL7, had the highest group mean concordance based on K = 2, cluster analysis was performed to obtain two two clusters, with 153 persons for AIG-high risk and 141 persons for AIG-low risk (Fig. 6A). Analysis

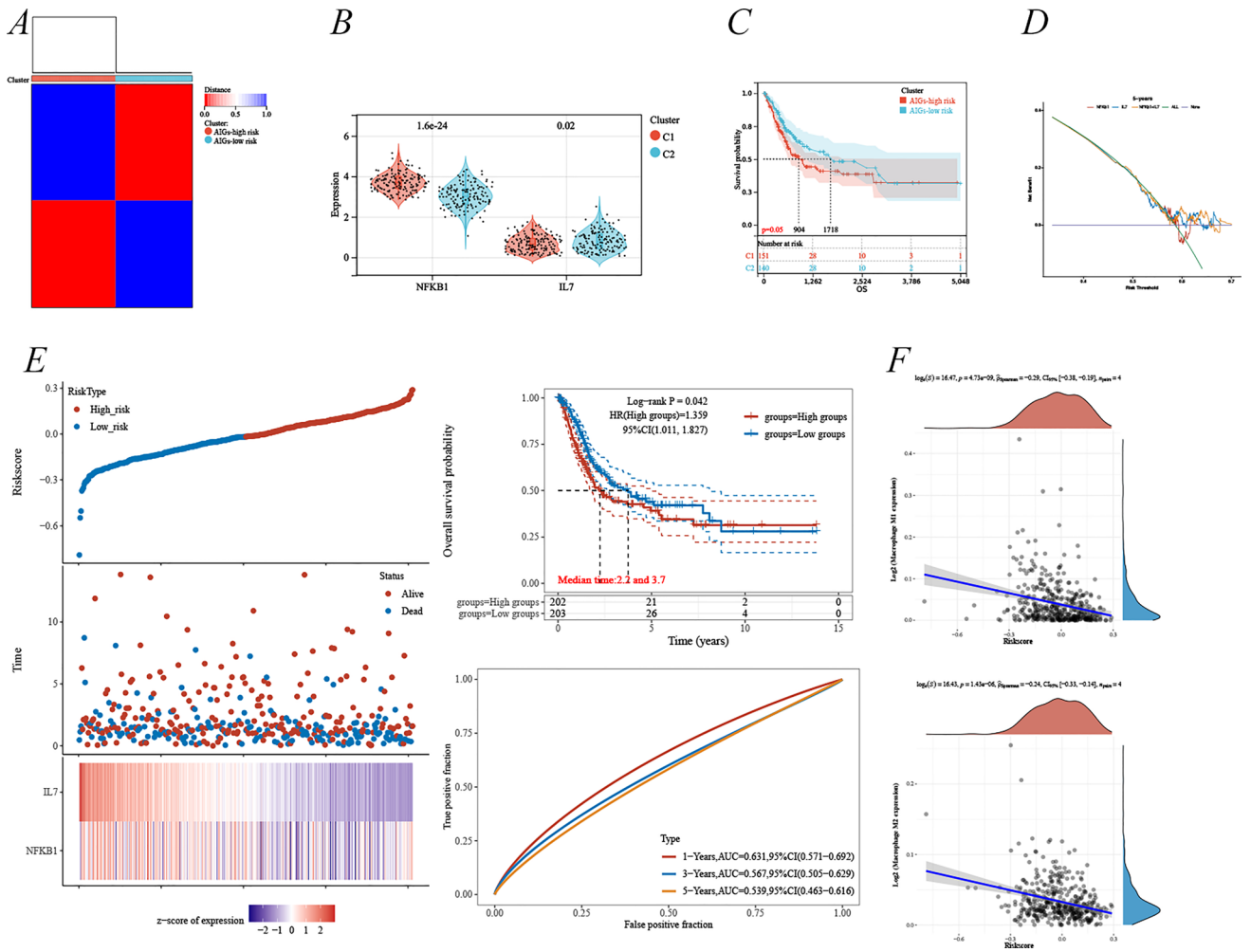

Fig. 6 Prognostic risk model for the combination of NFKB1 and IL7. **A** Heat map at K = 2 with 153 AIGs-high and 141 AIGs-low; **B** Differential expression of NFKB1 and IL7 in different clusters; **C** OS under clusters; **D** DCA curve analysis of NFKB1, IL7 and risk prognostic model; **E** Distribution of risk scores, survival of TCGA-BLCA patients status and heat map of hub AIGs, as well as overall survival and 1,3,5-year diagnostic AUC curves; **F** Correlation of the risk prognosis model with macrophage M1 and M2 polarization

of expression differences by clusters suggested that NFKB1 expression was higher and IL7 expression was lower in the AIG-high risk group relative to the AIG-low risk group (Fig. 6B). Combined with the OS results, patients with the AIG-high risk cluster had a significantly shorter OS (Fig. 6C), and therefore the AIG-high risk cluster (C1) was identified as the carcinogenic group, while the AIG-low risk cluster (C2) was the carcinogenic group. Cox regression analysis was used to construct a risk prognostic model based on NFKB1 and IL7 to obtain the optimal model AIC = 1884.9481 and Riskscore = (0.0581)*NFKB1 + (− 0.2285)*IL7. Analysis of the relationship between NFKB1-IL7 and survival status of BLCA patients showed that the high risk group had a lower number of survival states and relatively lower NFKB1 and IL7 expression (Fig. 6E). Analysis in the TCGA-BLCA cohort suggested that OS was shorter in the high risk group (Fig. 6E), and that the ROC-1, 3- and 5-year OS were 0.631, 0.567 and 0.539 respectively (Fig. 6E). The DCA curve further showed that the combined prognostic model of NFKB1 and IL7 had more application and better prognosis than the single gene prediction model (Fig. 6D). The prognostic model was then explored for immune correlation by the quanTIseq algorithm, which revealed a significant negative correlation with macrophage M1 and macrophage M2 expression (Fig. 6F).

3.6 Characterization of differential expressed genes and associated pathways in different clusters

To explore the molecular mechanisms underlying the differences in prognosis between the different clusters, 123 genes were identified, of which 54 were up-regulated and 69 were down-regulated (FC ≥ 1, $p < 0.05$) in the two clusters (Fig. 7A, B). KEGG analysis of the different genomes suggested that up-regulated genes were clustered

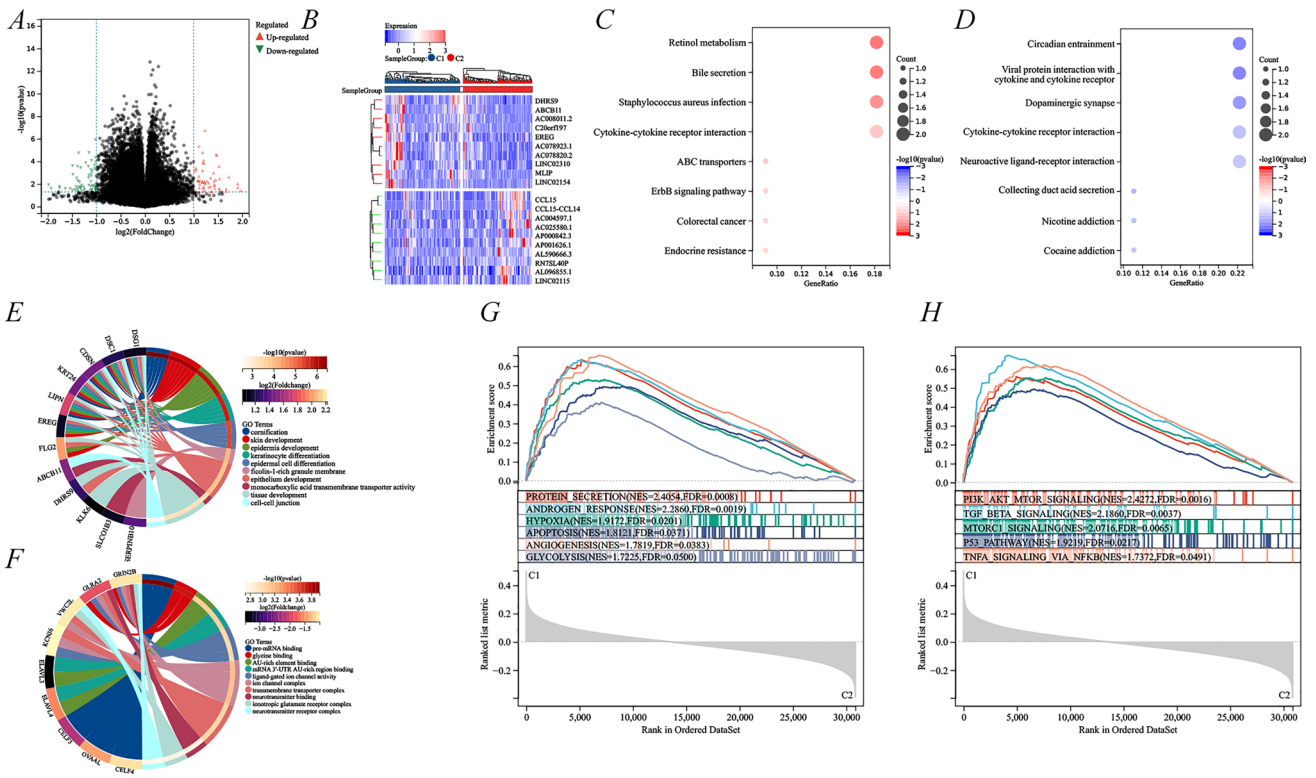

Fig. 7 Identification of differential expressed genes and pathway identification in different clusters. **A**, **B** Volcano and heat maps of DEGs in different clusters; KEGG analysis of up-regulated (**C**) and down-regulated (**D**) DEGs. GO analysis of up-regulated (**E**) and down-regulated (**F**) DEGs. **G**, **H** GSEA analysis of DEGs

in retinol metabolism, bile secretion and cytokine-cytokine receptor interaction (Fig. 7C); down-regulated genes were enriched in circadian entrainment, dopaminergic synapse and dopaminergic synapse, dopaminergic synapse and cytokine-cytokine receptor interaction (Fig. 7D). GO analysis revealed that up-regulated gene aggregation was involved in epidermal cell differentiation, cell junction and monocarboxylic acid transmembrane transporter activity (Fig. 7E). The down-regulated genes were enriched in premrna binding, ion channel complex and transmembrane transporter complex (Fig. 7E). Moreover, GSEA analysis further showed that AIG-high risk (C1) and AIG-low risk clusters (C2) on HYPOXIA, APOPTOSIS, ANGIOGENESIS, GLYCOLYSIS and signaling pathways (such as PI3K_AKT_MTOR_SIGNALING, TGF_BETA_SIGNALING, P53_PATHWAY, TNFA_SIGNALING_VIA_NFKB, etc.) had significant differences (Fig. 7G, H), which might be the underlying mechanism that leads to the different prognosis.

3.7 Exploration of the landscape of mutations and immune infiltration in different clusters

Through somatic mutation maps, this study found significant differences in gene mutations of AIG-high risk (C1) and AIG-low risk cluster (C2). The top 10 mutant genes of AIG-high risk cluster were TP53, TTN, KMT2D, MUC16, KDM6A, ARID1A, PIK3CA, KMT2C, SYNE1 and ZFHX4 (Fig. 8A). The AIG-low risk cluster were TP53, TTN, KMT2D, KDM6A, MUC16, ARID1A, SYNE1, RB1, HMCN1 and PIK3CA (Fig. 8B). Among them, the mutation rate of hub genes (TP53, TTN) was significantly lower in the AIG-high risk cluster than AIG-low risk cluster. Subsequently, based on the possibility that AIGs may regulate immune response activation or silencing, the tumor immune microenvironment was assessed by xCELL, TIMER, quanTIseq, CIBERSORT and EPIC algorithms under different clusters, and neutrophils were found to be significantly high in the AIG-high risk cluster (C1) in multiple algorithms (Fig. 9A–E), and CD4 T cells, CD8 T cells and DC cells, among others, differed in the different clusters (Fig. 9A–E).

Fig. 8 Gene mutations in different clusters. Visualization of the first 10 mutated genes in the AIGs clusters, **A** AIGs-high group; **B** AIGs-low group

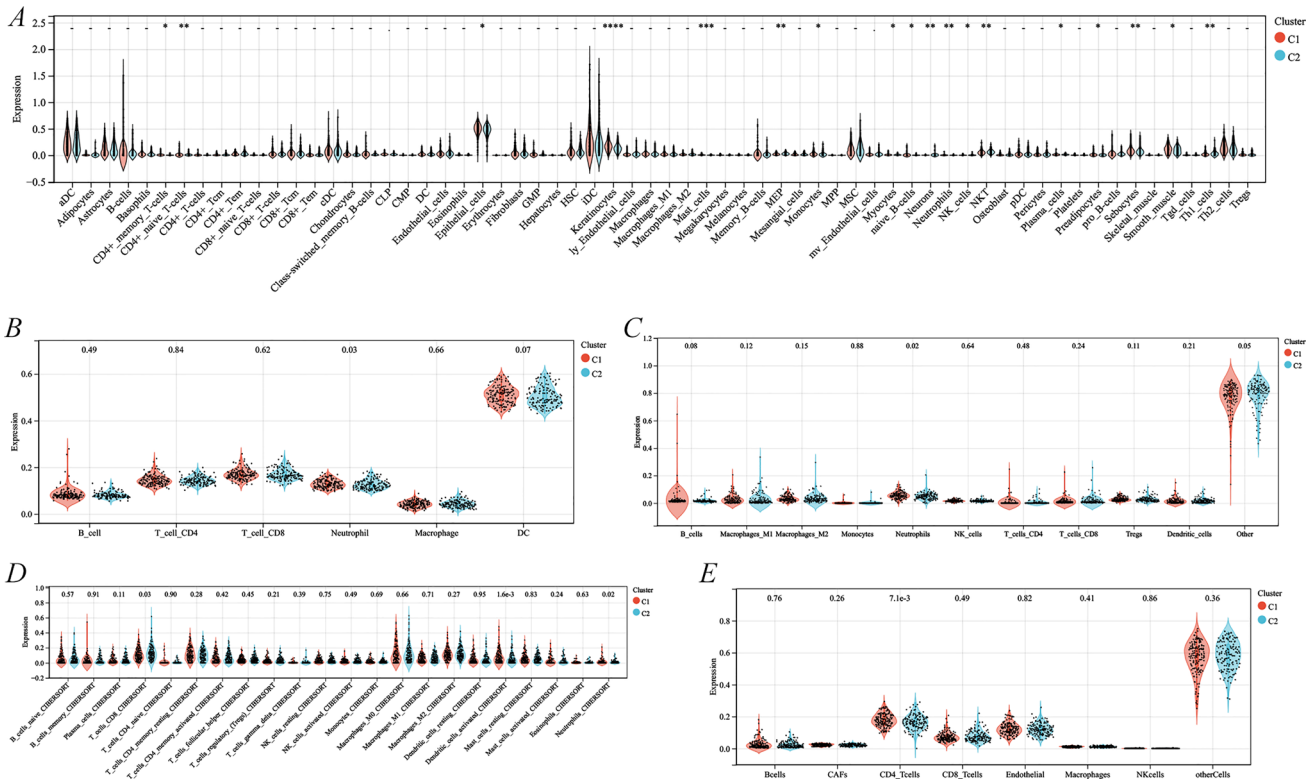

Fig. 9 Immune infiltration landscape under five algorithms in different clusters. **A** xCELL algorithm; **B** TIMER algorithm; **C** quanTIseq algorithm; **D** CIBERSORT algorithm; **E** EPIC algorithm. C1 is the AIGs-high group and C2 is the AIGs-low group

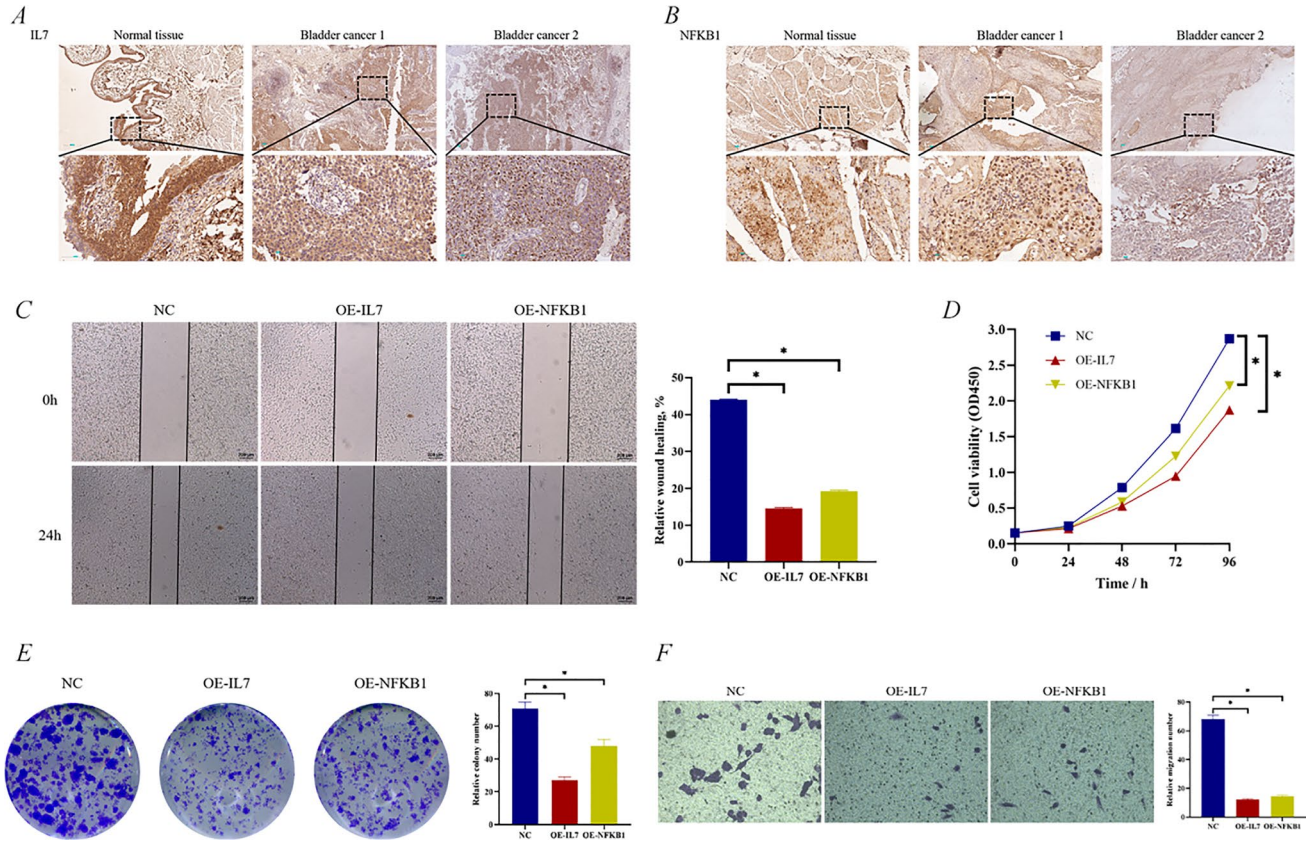

Fig. 10 IL7 and NFKB1 were proved to influence bladder cancer progression. **A** IL7 immunohistochemistry; **B** NFKB1 immunohistochemistry; **C** Scratch tests; **D** CCK8 assay; **E** clone formation assay; **F** transwell assay

3.8 Verification of IL7 and NFKB1 in BCa by cell phenotype and immunohistochemistry

Immunohistochemical experiments of bladder cancer patients in our medical center showed that both IL7 and NFKB1 were underexpressed in tumor tissues (Fig. 10A, B), and the conclusion was consistent with the above bioinformatics analysis results. Then, the relative wound healing rate of cells was found to be significantly lower after OE-IL7 and OE-NFKB1 by cell scratch assay (Fig. 10C). CCK8 experiments suggested weakened cell proliferation after OE-IL7 and OE-NFKB1 (Fig. 10D). In addition, the number of cell clones decreased after OE-IL7 and OE-NFKB1, compared with the NC group (Fig. 10E). Moreover, the cell migration ability was decreased after OE-IL7 and OE-NFKB1 (Fig. 10F). Collectively, the above studies further confirmed IL7 and NFKB1 as anti-oncogenes in BCa.

4 Discussion

The prevalence and mortality of bladder cancer is gradually increasing with an ageing population, of which there will be approximately 550,000 new cases worldwide in 2020 and 85,694 new cases in China. Since 1976, Bacillus Calmette-Guerin (BCG) bladder instillation has been used to treat BLCA, which was shown to be immunogenic [19]. Subsequently, immune checkpoint inhibitors (ICIs) and cisplatin-based neoadjuvant chemotherapy had both offered new prospects for the bladder cancer therapy, but a large number of patients still did not respond to immunotherapy or chemotherapy and had a poor prognosis [20, 21]. Immunosenescence was considered to be a major cause of tumourigenesis, which directly contributed to the immune surveillance and immunosuppression evasion in the tumor microenvironment [22, 23]. Therefore, exploring aging-immune-related mechanisms within BLCA and seeking new prognostic markers and immunotherapeutic targets will be effective in improving disease outcomes and prevention in the elderly.

Recent studies have increasingly focused on the role of senescence in bladder cancer, for example, Xia et al. found that berberine could induce bladder cancer cell senescence by inhibiting the Janus kinase 1 (JAK1)- STAT3 signalling pathway and increasing the regulation of miR-17-5p [24]; SENEX, a newly identified senescence gene, could promote the accumulation of regulatory T cells (Treg) in the urine of elderly bladder cancer patients [25]; and, cullins-1 regulator (ROC1) could promote NMIBC progression through anti-aging [26].

In this study, among 145 potentially bladder cancer-related prognostic aging-immune related genes, NFKB1 and IL7 were finally identified as the most valuable hub AIGs by differential expression, prognostic analysis and clinicopathological correlation analysis. This study found that NFKB1 and IL7 were significantly under-expressed in advanced age patients (> 70 years) and that the diagnostic AUC curves for NFKB1 and IL7 were significantly higher when combined with age grouping compared to independent prediction, which indicated that NFKB1 and IL7 are significantly correlated with age in bladder cancer and play an important role in patient aging and disease prognosis. Subsequently, immunocorrelation analysis of NFKB1 and IL7 revealed a significant association between NFKB1 and TMB scores and ICB response, and NFKB1 and IL7 were associated with various immune checkpoint-related genes and immune infiltrating cells. This suggested that these genes, especially NFKB, could be potential targets for immunotherapy and that the use of NFKB1 or IL7 as specific agents as "immune tonic" or adjuvant agents could bring a new change to the current status of bladder cancer immunotherapy. Finally, this study performed a cluster analysis for hub AIGs in BLCA and found that NFKB1 expression was higher and IL7 expression was lower in the AIG-high risk cluster, as well as patients had significantly shorter OS. The risk prognostic model was constructed using Cox regression analysis with Riskscore = (0.0581)*NFKB1 + (− 0.2285)*IL7 and found that this model was significantly negatively correlated with macrophage M1 and macrophage M2 expression. Additionally, for the different clusters, it was further found that the mutation rate of hub genes (TP53, TTN) was significantly lower and neutrophils were significantly higher in the AIG-high risk cluster, as well as CD4 T cells, CD8 T cells and DC cells were also differently abundant in the different clusters.

The present study was the first to identify NFKB1 and IL7 as the most hub AIGs in BLCA. NFKB1 was commonly described as promoting inflammation-associated cancer, but the anti-inflammatory p50 homodimer was also a tumour suppressor. Related studies confirmed that $Nfkb1^{-/-}$ mice had defects in spleen structure, B-cell proliferation and antibody responses, and were more susceptible to bacterial and helminthic pathogens due to inappropriate and ineffective T-cell responses [27, 28]. Furthermore, it had been shown that ageing was caused by a reduction in p50 homodimer levels and a p50:RelA heterodimer shift [29], and in the $Nfkb1^{-/-}$ mouse model chronic inflammation was found to lead to increased telomere damage, creating the senescence microenvironment that exacerbated the degree of inflammation and ultimately accelerated senescence through an inflammatory senescence-associated secretory phenotype [29]. Currently, NFKB1 has been less studied in bladder cancer and only NFKB1 promoter ins/deletion polymorphism was found to be a potential molecular marker for the risk of superficial bladder cancer recurrence [30], and the NFKB1 promoter −94 ins/del ATTG polymorphism might be associated with the etiology of bladder cancer in the Chinese population [31]. IL7 is a member of the common gamma chain (gamma c-cd132) cytokine family, and the relevance of IL7 to immunosenescence was first detailed in a review by Larrick [32]. Relevant studies had revealed by RT-PCR that IL-7 expression was significantly reduced in the elderly group compared to the middle-aged group [33], and the Leiden Longevity Research Group observed that the offspring of the elderly population did not show the expected age-related reduction in peripheral naïve T cells [34], thus the reduction in IL-7 signalling might somehow protect naïve T cells in favour of the biological age and health status of the elderly. Moreover, IL7 played an important role in B-lymphocyte production, T-lymphocyte production and thymic degeneration [32]. However, there are no studies to explore the functions and mechanisms associated with IL7 in bladder cancer. Interestingly, Professor Sung-Kwon Moon's study suggested a correlation between NFKB1 and IL7, with its demonstration that p27KIP1 was involved in ERK1/2-mediated MMP-9 expression through activation of NFKB binding in IL-7-induced migration and invasion of 5637 cells [35]. The above analysis indicated that NFKB1 and IL7 might play extremely important roles in aging-immune related functions, however their respective aging-immune mechanisms with bladder cancer had not been explored in the current academic community. Consequently, there is great potential for research into NFKB1 and IL7 in bladder cancer, which may provide new prognostic markers and immunotherapeutic targets, and effectively improve the high incidence and mortality in the ageing society.

Unfortunately, due to clinical, experimental and financial limitations, this study did not explore the specific mechanisms of IL7 and NFKB1 in bladder cancer and establish a large clinical prospective cohort to validate the practical application of the prognostic model. It was hoped that, when the conditions allowed, our center would be able to carry out various basic experiments, large clinical prospective cohorts, and related targeted drug studies on IL7 and NFKB1 to deeply explore their roles in bladder cancer.

5 Conclusion

In this study, comprehensive bioinformatics analysis was performed to obtain hub aging-immune related genes, including NFKB1 and IL7, which were significantly correlated with patient clinicopathological features, immune microenvironment, immunotherapeutic response, ferroptosis and m6A methylation in BLCA. Subsequent cluster analysis revealed that the AIG-high risk cluster was pro-cancer and had lower mutation rates of key genes (TP53, TTN) and higher neutrophil content. Moreover, the risk prognostic model was constructed by Cox regression analysis with Riskscore = (0.0581)*NFKB1 + (− 0.2285)*IL7. Finally, immunohistochemistry of patients confirmed that IL7 and NFKB1 were underexpressed in bladder cancer, and the proliferation and migration ability of tumor cells were significantly decreased after overexpression of these genes. This study contributes to an in-depth exploration of the aging-immune related mechanisms and the search for new prognostic markers and immunotherapeutic targets to effectively improve disease outcome and prevention.

Acknowledgements No.

Author contributions All authors participated in the design, interpretation of the studies and analysis of the data and review of the manuscript. NH-C and F-C contributed to this manuscript and should be considered as the first authors. They were jointly responsible for the study design, data extraction and analysis as well as the writing and revision of the manuscript. JC-Z and N-L were considered co-responding authors, who were responsible for the design of the study idea and review of the manuscript.

Funding This study was supported by Nanjing Health Technology Development Project (YKK24273).

Data availability This study was based on RNAseq and clinical information from the public database TCGA-BLCA disease cohort (https://portal.gdc.cancer.gov/). Relevant data for the secondary analysis were available in the manuscript or in the Supplementary information document.

Declarations

Ethics approval and consent to participate All subjects gave their informed consent for inclusion before they participated in the study. The study was conducted in accordance with the Declaration of Helsinki. The protocol was approved by the Clinical Ethics Committee of Zhongda Hospital Affiliated to Southeast University.

Competing interests The authors declare no competing interests.

Open Access This article is licensed under a Creative Commons Attribution-NonCommercial-NoDerivatives 4.0 International License, which permits any non-commercial use, sharing, distribution and reproduction in any medium or format, as long as you give appropriate credit to the original author(s) and the source, provide a link to the Creative Commons licence, and indicate if you modified the licensed material. You do not have permission under this licence to share adapted material derived from this article or parts of it. The images or other third party material in this article are included in the article's Creative Commons licence, unless indicated otherwise in a credit line to the material. If material is not included in the article's Creative Commons licence and your intended use is not permitted by statutory regulation or exceeds the permitted use, you will need to obtain permission directly from the copyright holder. To view a copy of this licence, visit http://creativecommons.org/licenses/by-nc-nd/4.0/.

References

1. Sung H, et al. Global Cancer Statistics 2020: GLOBOCAN estimates of incidence and mortality worldwide for 36 cancers in 185 countries. CA Cancer J Clin. 2021;71:209–49. https://doi.org/10.3322/caac.21660.
2. Babjuk M, et al. EAU guidelines on non-muscle-invasive urothelial carcinoma of the bladder: update 2013. Eur Urol. 2013;64:639–53. https://doi.org/10.1016/j.eururo.2013.06.003.
3. Millan-Rodriguez F, et al. Primary superficial bladder cancer risk groups according to progression, mortality and recurrence. J Urol. 2000;164:680–4. https://doi.org/10.1016/s0022-5347(05)67280-1.
4. Shariat SF, et al. The effect of age and gender on bladder cancer: a critical review of the literature. BJU Int. 2010;105:300–8. https://doi.org/10.1111/j.1464-410X.2009.09076.x.
5. Freedman ND, Silverman DT, Hollenbeck AR, Schatzkin A, Abnet CC. Association between smoking and risk of bladder cancer among men and women. JAMA. 2011;306:737–45. https://doi.org/10.1001/jama.2011.1142.
6. Coussens LM, Werb Z. Inflammation and cancer. Nature. 2002;420:860–7. https://doi.org/10.1038/nature01322.
7. Wallis CJ, et al. Second malignancies after radiotherapy for prostate cancer: systematic review and meta-analysis. BMJ. 2016;352: i851. https://doi.org/10.1136/bmj.i851.
8. Carlo MI, et al. Cancer susceptibility mutations in patients with urothelial malignancies. J Clin Oncol. 2020;38:406–14. https://doi.org/10.1200/JCO.19.01395.

9. Ritch CR, et al. Use and validation of the AUA/SUO risk grouping for nonmuscle invasive bladder cancer in a contemporary cohort. J Urol. 2020;203:505–11. https://doi.org/10.1097/JU.0000000000000593.
10. Doherty AP, Trendell-Smith N, Stirling R, Rogers H, Bellringer J. Perivesical fat necrosis after adjuvant intravesical chemotherapy. BJU Int. 1999;83:420–3. https://doi.org/10.1046/j.1464-410x.1999.00951.x.
11. Brausi M, et al. Side effects of Bacillus Calmette-Guerin (BCG) in the treatment of intermediate- and high-risk Ta, T1 papillary carcinoma of the bladder: results of the EORTC genito-urinary cancers group randomised phase 3 study comparing one-third dose with full dose and 1 year with 3 years of maintenance BCG. Eur Urol. 2014;65:69–76. https://doi.org/10.1016/j.eururo.2013.07.021.
12. Stein R. Campbell Walsh Wein urology. Aktuel Urol. 2021;52:25–25. https://doi.org/10.1055/a-1307-2419.
13. Schultzel M, et al. Late age (85 years or older) peak incidence of bladder cancer. J Urol. 2008;179:1302–5. https://doi.org/10.1016/j.juro.2007.11.079. (**discussion 1305-1306**).
14. Herr HW. Age and outcome of superficial bladder cancer treated with bacille Calmette-Guerin therapy. Urology. 2007;70:65–8. https://doi.org/10.1016/j.urology.2007.03.024.
15. Joudi FN, Smith BJ, O'Donnell MA, Konety BR. The impact of age on the response of patients with superficial bladder cancer to intravesical immunotherapy. J Urol. 2006;175:1634–9. https://doi.org/10.1016/S0022-5347(05)00973-0. (**discussion 1639-1640**).
16. Palmer S, Albergante L, Blackburn CC, Newman TJ. Thymic involution and rising disease incidence with age. Proc Natl Acad Sci USA. 2018;115:1883–8. https://doi.org/10.1073/pnas.1714478115.
17. Santoro A, Bientinesi E, Monti D. Immunosenescence and inflammaging in the aging process: age-related diseases or longevity? Ageing Res Rev. 2021;71: 101422. https://doi.org/10.1016/j.arr.2021.101422.
18. Zhou R, et al. An immunosenescence-related gene signature to evaluate the prognosis, immunotherapeutic response, and cisplatin sensitivity of bladder cancer. Dis Markers. 2022;2022:2143892. https://doi.org/10.1155/2022/2143892.
19. Morales A, Eidinger D, Bruce AW. Intracavitary Bacillus Calmette-Guerin in the treatment of superficial bladder tumors. J Urol. 1976;116:180–3. https://doi.org/10.1016/s0022-5347(17)58737-6.
20. Patel VG, Oh WK, Galsky MD. Treatment of muscle-invasive and advanced bladder cancer in 2020. CA Cancer J Clin. 2020;70:404–23. https://doi.org/10.3322/caac.21631.
21. Yin M, et al. Neoadjuvant chemotherapy for muscle-invasive bladder cancer: a systematic review and two-step meta-analysis. Oncologist. 2016;21:708–15. https://doi.org/10.1634/theoncologist.2015-0440.
22. Feehan J, Tripodi N, Apostolopoulos V. The twilight of the immune system: the impact of immunosenescence in aging. Maturitas. 2021;147:7–13. https://doi.org/10.1016/j.maturitas.2021.02.006.
23. Fane M, Weeraratna AT. How the ageing microenvironment influences tumour progression. Nat Rev Cancer. 2020;20:89–106. https://doi.org/10.1038/s41568-019-0222-9.
24. Xia Y, et al. Berberine suppresses bladder cancer cell proliferation by inhibiting JAK1-STAT3 signaling via upregulation of miR-17-5p. Biochem Pharmacol. 2021;188: 114575. https://doi.org/10.1016/j.bcp.2021.114575.
25. Chen T, et al. A novel cellular senescence gene, SENEX, is involved in peripheral regulatory T cells accumulation in aged urinary bladder cancer. PLoS ONE. 2014;9: e87774. https://doi.org/10.1371/journal.pone.0087774.
26. Wang W, et al. Knockdown of regulator of cullins-1 (ROC1) expression induces bladder cancer cell cycle arrest at the G2 phase and senescence. PLoS ONE. 2013;8: e62734. https://doi.org/10.1371/journal.pone.0062734.
27. Sha WC, Liou HC, Tuomanen EI, Baltimore D. Targeted disruption of the p50 subunit of NF-kappa B leads to multifocal defects in immune responses. Cell. 1995;80:321–30. https://doi.org/10.1016/0092-8674(95)90415-8.
28. Artis D, et al. Differential requirement for NF-kappa B family members in control of helminth infection and intestinal inflammation. J Immunol. 2002;169:4481–7. https://doi.org/10.4049/jimmunol.169.8.4481.
29. Jurk D, et al. Chronic inflammation induces telomere dysfunction and accelerates ageing in mice. Nat Commun. 2014;2:4172. https://doi.org/10.1038/ncomms5172.
30. Riemann K, et al. Insertion/deletion polymorphism in the promoter of NFKB1 as a potential molecular marker for the risk of recurrence in superficial bladder cancer. Int J Clin Pharmacol Ther. 2007;45:423–30. https://doi.org/10.5414/cpp45423.
31. Li P, et al. Functional promoter -94 ins/del ATTG polymorphism in NFKB1 gene is associated with bladder cancer risk in a Chinese population. PLoS ONE. 2013;8: e71604. https://doi.org/10.1371/journal.pone.0071604.
32. Nguyen V, Mendelsohn A, Larrick JW. Interleukin-7 and immunosenescence. J Immunol Res. 2017;2017:4807853. https://doi.org/10.1155/2017/4807853.
33. Passtoors WM, et al. IL7R gene expression network associates with human healthy ageing. Immun Ageing. 2015;12:21. https://doi.org/10.1186/s12979-015-0048-6.
34. Derhovanessian E, et al. Hallmark features of immunosenescence are absent in familial longevity. J Immunol. 2010;185:4618–24. https://doi.org/10.4049/jimmunol.1001629.
35. Park SL, Lee EJ, Kim WJ, Moon SK. p27KIP1 is involved in ERK1/2-mediated MMP-9 expression via the activation of NF-kappaB binding in the IL-7-induced migration and invasion of 5637 cells. Int J Oncol. 2014;44:1349–56. https://doi.org/10.3892/ijo.2014.2290.

Publisher's Note Springer Nature remains neutral with regard to jurisdictional claims in published maps and institutional affiliations.